

Influence of Contact Angle on Soil–Water Characteristic Curve with Modified Capillary Rise Method

Zhen Liu, Xiong (Bill) Yu, and Lin Wan

The contact angle quantifies physicochemical interactions at the liquid–solid interface and is therefore critical to many physical processes that involve the interaction of soil and water. In geotechnical engineering, such interactions are the basis for the formulation of the soil–water characteristic curve (SWCC). However, the role of the contact angle in SWCCs has not been adequately recognized. A comprehensive study is reported on applying the capillary rise method (CRM) to measure the contact angles of soils. Analytical solutions to two forms of the Lucas–Washburn equation are presented to provide the theoretical basis for applying the CRM to soils. The disadvantages of conventional CRM analyses are demonstrated with experiments. A modified CRM was proposed on the basis of an analytical solution to a more complicated form of the Lucas–Washburn equation. This modified CRM exhibited reliable performance on numerous specimens made of a subgrade soil and a silicon dioxide sand. Testing procedures were designed and strictly followed, and innovative apparatuses for the preparation, transport, and accommodation of soil specimens were fabricated to ensure repeatability. For the modified CRM, experimental results for virgin specimens demonstrated good repeatability, and for sieved soils, clear trends were observed in the variations of contact angle with respect to pore size. Contact angles much greater than zero were observed for all tested specimens; this finding contradicts the assumption of perfect wettability in previous SWCC studies. In addition, it was demonstrated that neglecting the variations of contact angles with respect to pore radius could result in significant errors in SWCC construction.

Contact angle, or more specifically water–air contact angle, is an intrinsic property of solid–liquid–gas systems such as soils (1). It is of great significance in many physical processes involving the interaction of soil and water (2, 3). For example, it is critical to water infiltration, redistribution, groundwater recharge, solute transport in unsaturated zones, compaction and aeration in variably saturated soils, and temperature-induced water redistribution (4, 5) because this property quantifies the ability of a liquid to spread on another solid (6).

In geotechnical engineering, the importance of this property primarily lies in the fact that the contact angle is essential to the

establishment of the soil–water characteristic curve (SWCC), which is believed to be one of the fundamental concepts in unsaturated soil mechanics (7). The SWCC depends on both the soil matrix tomography (i.e., pore-size distribution) and the surface physical chemistry (i.e., contact angle). Although the pore-size distribution has been extensively studied for SWCCs, the contact angle is usually assumed to be a constant, mostly zero, for simplicity in view of the high surface energy of soil minerals (4, 7, 8). However, these assumptions have rarely been validated by experimental evidence. In fact, a varying (nonzero) contact angle with respect to various factors, such as water potential, roughness, and temperature, has been frequently reported by researchers outside of the geotechnical engineering area, such as soil scientists, agricultural engineers, and physical chemists (9–13). Therefore, a closer look into the contact angle is necessary for further understanding and formulating SWCCs in geotechnical applications.

Various methods have been proposed for the measurement of contact angles of soils, for example, water drop penetration time (14), molarity of an ethanol droplet (15, 16), and flotation time (17, 18). More recently, the capillary rise method (CRM) (19), sessile drop method (20), and Wilhelmy plate method (21) were developed. Among these methods, the CRM based on the Lucas–Washburn equation (22, 23) is designated for hydrophilic soils; the method applies to common types of soils in geotechnical engineering. One distinct advantage of this method is that it is capable of assessing the average contact angle of a bulk soil rather than that of several layers of the soil near the surface. This average contact angle, which is called the apparent contact angle, is different from the intrinsic contact angle between water and a flat, smooth, mineral interface. Rather, it represents the average contact angle of a conceptualized bundle of cylindrical capillaries (BCC) (24); this conceptualization of soil is also used by most SWCC formulations. Therefore, the CRM is by nature suitable for SWCC studies.

Despite the development of the Lucas–Washburn equation since the 1920s (22, 23), the CRM for porous materials based on this equation was not extensively investigated until the 1990s (19). For this reason there have only been a few attempts to apply this method to soils. The earliest effort was the study by Letey et al. on the measurement of liquid–solid contact angles in soils based on a theory equivalent to the Lucas–Washburn equation (6). Siebold et al. applied the CRM to silica flour and calcium carbonate by measuring both the height (by a scale) and mass (by the Krüss 12 tensiometer) of imbibed liquids (25). Michel et al. measured the wettability of partly decomposed peats with the Krüss 12 tensiometer on the basis of the CRM, in which the tortuosity of the capillaries was considered (26). Abu-Zreig et al. made a simple application of the CRM for measuring contact angles between soils and various test liquids (27).

Z. Liu, Bingham 256, X. Yu, Bingham 206, and L. Wan, Bingham 259, Department of Civil Engineering, Case Western Reserve University, 2104 Adelbert Road, Cleveland, OH 44106-7201. Corresponding author: X. Yu, xxy21@case.edu.

Transportation Research Record: Journal of the Transportation Research Board, No. 2349, Transportation Research Board of the National Academies, Washington, D.C., 2013, pp. 32–40.
DOI: 10.3141/2349-05

Goebel et al. claimed that their study was the first one that applied the CRM to soil aggregates (10). Ramirez-Flores et al. followed Goebel's method (10) for measuring the contact angles of intact soil aggregates, packing of intact aggregates, and packing of crushed aggregates of nine topsoils and three humus subsoils (13).

This study presents a comprehensive look at applying the CRM to measure the contact angle of hydrophilic soils. To the authors' knowledge, this study is among the first to investigate CRMs for geotechnical engineering research, in the hope of promoting further research on SWCCs. The derivations of analytical solutions to two forms of the Lucas–Washburn equation are presented to lay down the theoretical basis for applying the CRM to soils; this basis is currently lacking. Measures were taken to overcome several difficulties that prevent accurate contact angle measurements with the CRM: (a) external meniscus elimination with a specially designed self-fabricated tube, (b) consistency in sample quality and repeatability of experiments with specially designed soil specimen preparation procedures, and (c) avoidance of subjective factors with automatic data processing. Experiments and data analyses identified disadvantages of the conventional CRM method, from which a modified CRM method is proposed and validated. Contact angles are measured for specimens made of two types of soils, either virgin or sieved. The implications of the experiment results on SWCC studies are discussed.

THEORY

Four types of forces are involved in the dynamic process of capillary rise in a cylindrical tube or a capillary, including surface tension, inertial force, viscous force, and gravity. The governing equation is obtained by ensuring the equilibrium of imbibed liquid by allowing for these forces (28, 29):

$$\underbrace{2\pi r\gamma \cos(\theta)}_{\text{surface tension}} - \underbrace{\rho\pi r^2 \frac{\partial}{\partial t} \left[h(t) \frac{\partial h(t)}{\partial t} \right]}_{\text{inertial force}} - \underbrace{8\pi\eta h(t) \frac{\partial h(t)}{\partial t}}_{\text{viscous force}} - \underbrace{\rho\pi r^2 g h(t)}_{\text{gravity}} = 0 \quad (1)$$

where

- r = radius of tube;
- γ = surface tension of interface between solid and test (imbibed) liquid;
- θ = water–air contact angle;
- t = time;
- $h(t)$ = height of capillary rise at time t ;
- η, ρ = dynamic viscosity and density of test liquid, respectively; and
- g = gravitational acceleration.

This equation can be simplified:

$$B - A(hh')' - Chh' - Dh = 0 \quad (2)$$

where

- $A = \rho\pi r^2$,
- $B = 2\pi r\gamma \cos(\theta)$,
- $C = 8\pi\eta$,
- $D = \rho\pi r^2 g$, and
- h' = derivative of h .

Equation 1 is the most up-to-date form of the Lucas–Washburn equation based on modifications to the original ones with and without gravity (30). When this equation is extended to porous materials such as soils, a porous medium is conceptualized as a BCC. For the dynamics of capillary rise, the original BCC of different radii was then equivalently viewed as another one of the same radius (31). This radius is called the effective radius or average radius. The Lucas–Washburn equation is assumed to be valid for the capillary rise in every capillary within the equivalent bundle.

However, there is no analytical solution for Equation 1. Preliminary investigations in the current study indicated that direct curve fitting with the foregoing ordinary differential equation (ODE) to experimental data requires an optimization capacity far beyond what is currently available. So, in the current stage, a feasible strategy is to obtain an analytical solution to a simplified form of the complete Lucas–Washburn equation and then to perform curve fitting with the analytical solution. This strategy is actually that used by previous CRM studies.

Conventional CRM Based on Simplified Lucas–Washburn Equation

The influences of inertia and gravity were neglected in most of the previous CRM studies. Consequently, a simplified Lucas–Washburn equation is obtained in the following form:

$$\underbrace{2\pi r\gamma \cos(\theta)}_{\text{surface tension}} - \underbrace{8\pi\eta h(t) \frac{\partial h(t)}{\partial t}}_{\text{viscous force}} = 0 \quad B - Chh' = 0 \quad (3)$$

The analytical solution to this simplified Lucas–Washburn equation predicts a linear relationship between the squared height of the imbibed liquid and time (19, 23):

$$h = \left(\frac{2B}{C} t \right)^{\frac{1}{2}} = \left(\frac{r\gamma \cos\theta}{2\eta} t \right)^{\frac{1}{2}} \quad (4)$$

It is possible that the height of the liquid front is not visible or that the liquid front does not accurately reflect the inner progression of the liquid in the porous material. Hence, the foregoing solution (height of capillary rise) is reformatted in the form of the imbibed mass (mass gain). An equivalent equation was then obtained; this equation was used by most CRM studies (conventional CRM) (25).

$$m = \left(\pi^2 r^5 N \cdot \frac{\rho^2 \gamma}{2\eta} \cdot \cos\theta \cdot t \right)^{\frac{1}{2}} \quad (5)$$

where N is the number of equivalent capillaries involved in a capillary rise process, and $\pi^2 r^5 N$ is usually referred to as the Washburn constant. The conventional CRMs require identifying a stage (viscous dominant) in which the simplified Lucas–Washburn equation can satisfactorily describe the dynamics of capillary rise (32). However, it is possible that such a stage is very short or even is not obvious. Even if there exists such a stage, a part of the m^2 - t curve where its tangent has the least slope variation needs to be identified for linear regression (25). Thus the implementation of the method could be very subjective. These two concerns were investigated with experiments and will be introduced later.

Modified CRM Based on Lucas–Washburn Equation Considering Gravity

To improve the conventional CRM, the influence of gravity is considered:

$$\underbrace{2\pi r \gamma \cos(\theta)}_{\text{surface tension}} - \underbrace{8\pi \eta h(t) \frac{\partial h(t)}{\partial t}}_{\text{viscous force}} - \underbrace{\rho \pi r^2 g h(t)}_{\text{gravity}} = 0 \quad (6)$$

An analytical solution to Equation 6 was obtained by using MATLAB:

$$h = \frac{B}{D} \left\{ 1 - W \left[\exp \left(-1 - \frac{D^2}{BC} t \right) \right] \right\} \quad (7)$$

where W is the Lambert W function; that is,

$$h = \frac{2\gamma \cos(\theta)}{\rho g r} \left\{ 1 - W \left[\exp \left(-1 - \frac{\rho^2 g^2 r^3}{16\gamma \eta \cos(\theta)} t \right) \right] \right\} \quad (8)$$

The solution is reformatted to describe the variation of mass:

$$m = \frac{2\pi r N \gamma \cos(\theta)}{g} \left\{ 1 - W \left[\exp \left(-1 - \frac{\rho^2 g^2 r^3}{16\gamma \eta \cos(\theta)} t \right) \right] \right\} \quad (9)$$

A piecewise equation proposed by Barry et al. was used to approximate the Lambert W equation in this study (33).

Application to Porous Materials

Czachor claimed that two features of porous materials should be responsible for the overestimation of contact angle in the application of the Lucas–Washburn equation to porous materials: cross section and tortuosity (34). According to the definition of the apparent contact angle (35, 36), the irregular characteristic has already been taken into account. So the contact angle of a porous medium measured with the CRM is the apparent contact angle considering roughness. However, tortuosity was not included in the definition of apparent contact angle. According to Czachor (34), the tortuosity τ is the ratio of the actual path taken by a moving liquid through pores, \tilde{h} , to the distance between the starting and final height, h (37, 38):

$$\tilde{h} = \tau h \quad (10)$$

The Lucas–Washburn equation taking into account tortuosity of the porous material is

$$\underbrace{2\pi \tilde{r} \gamma \cos(\tilde{\theta})}_{\text{surface tension}} - \underbrace{\rho \pi \tilde{r}^2 \frac{\partial}{\partial t} \left[\tilde{h}(t) \frac{\partial \tilde{h}(t)}{\partial t} \right]}_{\text{inertial force}} - \underbrace{8\pi \eta \tilde{h}(t) \frac{\partial \tilde{h}(t)}{\partial t}}_{\text{viscous force}} - \underbrace{\rho \pi \tilde{r}^2 g \tilde{h}(t)}_{\text{gravity}} = 0 \quad (11)$$

where \tilde{r} and $\tilde{\theta}$ are the effective pore radius and contact angle considering tortuosity, respectively. Equation 16 (presented later, in the discussion of Method 2) needs to be transformed in terms of the apparent capillary rise instead of the actual path to take advantage of the measured data:

$$\underbrace{2\pi \tilde{r} \gamma \cos(\tilde{\theta})}_{\text{surface tension}} - \underbrace{\rho \pi \tilde{r}^2 \tau^2 \frac{\partial}{\partial t} \left[h(t) \frac{\partial h(t)}{\partial t} \right]}_{\text{inertial force}} - \underbrace{8\pi \eta \tau^2 h(t) \frac{\partial h(t)}{\partial t}}_{\text{viscous force}} - \underbrace{\rho \pi \tilde{r}^2 g \tau h(t)}_{\text{gravity}} = 0 \quad (12)$$

Equation 12 can be simplified as follows:

$$\tilde{B} - \tilde{A}(hh')' - \tilde{C}hh' - \tilde{D}h = 0 \quad (13)$$

where

$$\begin{aligned} \tilde{A} &= \rho \pi \tilde{r}^2 \tau^2, \\ \tilde{B} &= 2\pi \tilde{r} \gamma \cos(\tilde{\theta}), \\ \tilde{C} &= 8\pi \eta \tau^2, \text{ and} \\ \tilde{D} &= \rho \pi \tilde{r}^2 g \tau. \end{aligned}$$

From the previous discussion, it is clear that the fitting functions for both conventional CRMs (Method 1) and the modified CRM (Method 2) need to be adjusted for tortuosity before their application. The adjusted governing equation (ODE), fitting functions, and desired fitting constants for height gain and mass gain, respectively, are summarized in Table 1. The term m_0 , which describes the mass absorbed on the balance before measurement, was added to the fitting functions (39).

MATERIALS AND METHOD

Method

Based on the fitting functions in Table 1, water and another reference liquid are usually used to obtain contact angles. The test liquid used for reference is usually an organic solvent with low surface energy, such as hexane or pentane. Considering the comparatively high surface energy of soil particles and low surface tension of the reference liquid, the contact angle between the reference liquid and a soil is approximately zero. Then the apparent contact angle between water and soils can be calculated by using Equations 14 and 15 with κ_J ($\kappa_{J,w}$ and $\kappa_{J,p}$) obtained by curve fitting.

$$\theta_1 = \arccos \left(\frac{\kappa_{1,w} \cdot \frac{\eta_w \rho_p^2 \gamma_p}{\eta_p \rho_w^2 \gamma_w}}{\kappa_{1,p}} \right) \quad (14)$$

$$\theta_2 = \arccos \left(\frac{\kappa_{2,w} \cdot \frac{\gamma_p}{\gamma_w}}{\kappa_{2,p}} \right) \quad (15)$$

where

$$\begin{aligned} \theta_J &= \text{contact angle obtained by Method } J; \\ \kappa_{J,p}, \kappa_{J,w} &= \text{constants pertaining to pentane and water, respectively;} \\ \rho_p, \gamma_p &= \text{density and surface tension of pentane, respectively;} \text{ and} \\ \rho_w, \gamma_w &= \text{density and surface tension of water, respectively.} \end{aligned}$$

The effective radius and number of capillaries were cancelled out.

Two types of experiments were conducted in this study. For the first type, duplicate soil specimens made of the same soil were tested. All of these specimens were prepared in the same way to ensure similarity among them. The measured m - t curves were fitted by using the fitting functions affiliated with different methods. In this way the suitability of these methods for analyzing capillary rise in soils

TABLE 1 ODEs, Fitting Functions, and Constants Containing Contact Angle

Method	Method 1	Method 2
ODE	$h = \left(\frac{2\tilde{B}}{\tilde{C}} t \right)^{\frac{1}{2}}$	$h = \frac{\tilde{B}}{\tilde{D}} \left\{ 1 - W \left[\exp \left(-1 - \frac{\tilde{D}^2}{\tilde{B}\tilde{C}} t \right) \right] \right\}$
Function	$h = (\kappa_1 t)^{1/2}$	$h = \kappa_2 \{ 1 - W[\exp(-1 - \alpha_2 t)] \}$
Constant	$\kappa_1 = \frac{2\tilde{B}}{\tilde{C}} = \frac{\tilde{r} \gamma \cos(\tilde{\theta})}{2\eta\tau^2}$	$\kappa_2 = \frac{\tilde{B}}{\tilde{D}} = \frac{2\gamma \cos(\tilde{\theta})}{\rho g \tilde{r} \tau}$
ODE	$m = \tilde{M} \left(\frac{2\tilde{B}}{\tilde{C}} t \right)^{\frac{1}{2}}$	$m = \frac{\tilde{B}\tilde{M}}{\tilde{D}} \left\{ 1 - W \left[\exp \left(-1 - \frac{\tilde{D}^2}{\tilde{B}\tilde{C}} t \right) \right] \right\}$
Function	$m = (\kappa_1 t)^{1/2}$	$m = \kappa_2 \{ 1 - W[\exp(-1 - \alpha_2 t)] \}$
Constant	$\kappa_1 = \frac{2\tilde{B}\tilde{M}^2}{\tilde{C}} = \frac{\rho^2 \pi^2 \tilde{r}^5 \gamma N^2 \cos(\tilde{\theta})}{2\eta\tau^2}$	$\kappa_2 = \frac{\tilde{B}\tilde{M}}{\tilde{D}} = \frac{2\pi \tilde{r} \gamma N \cos(\tilde{\theta})}{g\tau}$

NOTE: $\tilde{M} = \rho\pi\tilde{r}^2N$; α , β , κ are the combinations of the basic fitting constants, i.e., \tilde{A} , \tilde{B} , \tilde{C} , and \tilde{D} .

was tested. In the other type of experiment, the soils were sieved to obtain specimens of different particle sizes. The contact angles of these specimens were measured to investigate the variation of contact angle with respect to pore size as well as the relationship between contact angle and the SWCCs.

Materials

For test liquids, water (tap water) and pentane were used in this study. The density, surface tension, and viscosity of water are $1,000 \text{ kg/m}^3$, $71.79 \times 10^{-3} \text{ N/m}$, and $1.002 \times 10^{-3} \text{ N} \cdot \text{s/m}^2$, respectively; and those of pentane are 626.2 kg/m^3 , $15.82 \times 10^{-3} \text{ N/m}$, and $0.24 \times 10^{-3} \text{ N} \cdot \text{s/m}^2$, respectively. Two soils were used for both types of experiments: a typical Ohio subgrade soil (Soil A) and a silicon sand (Sand B). Table 2 shows the information regarding specimen number, particle size, density of Soil A and Sand B, and the results of the sieve analy-

ses conducted on the soils. Four specimens were prepared and tested for each specimen number, two of which were tested with water and the other two with pentane; the densities shown are average values.

All soil specimens were prepared by strictly following the same procedures to ensure their similarity. A soil was poured into a tube standing upright on a table from the same height as the top of the tube. After the upper surface of the soil reached the top of the tube, the tube was vibrated with a small vibrator at a frequency of 55 Hz for 60 s. A metallic tool with a base and a vertically protruding pipe was used to accommodate the tube while it was on the vibrator. All vibrated soil specimens were then put into a tube rack for transportation and testing. A tissue roll and a piece of plastic wrap were used to protect the specimen from any further disturbance and pollution. The densities of the specimens in Table 2 were used for quality control. This parameter was used for designing the procedures of specimen preparation. Also, any specimen whose density was significantly far from the average value was rejected.

TABLE 2 Properties of Specimens of Soil A and Sand B

Specimen	Sieve No.	Opening (μm)	Soil A		Sand B	
			Density ^a (g/cm^3)	Content ^b (%)	Density ^a (g/cm^3)	Content ^b (%)
1	20	840	1.10	16.21	1.43	60.02
2	40	420	1.06	19.69	1.38	20.76
3	50	300	1.02	13.38	1.35	5.19
4	60	250	0.98	5.38	1.31	7.27
5	70	210	0.98	6.92	1.30	3.35
6	80	180	0.96	6.89	1.23	1.69
7	120	125	0.94	7.77	1.23	1.74
8	140	105	0.88	7.44	na	na
9	170	90	0.73	8.02	na	na
10	200	75	0.77	8.49	na	na

NOTE: No. = number; na = not applicable.

^aDry density when tube is fully packed by soil before compaction by vibration.

^bPercentage of soil retained by sieve.

Apparatus

A K100 tensiometer was used for the contact angle measurements (40); its electronic balance instead of the built-in modules was employed. As shown in Figure 1, a self-fabricated tube filled with a soil was attached to the electronic balance with a clip. The rigid clip was used to reduce the time of self-stability for the electronic balance. A glass vessel containing a test liquid was placed on a lifting stage below the tube. During measurement, the stage moved up until it contacted the sieve glued at the bottom of the tube. The measurement of the m - t curve was triggered when a contact was detected.

The glass tubes are 44.5 mm high and have an inner diameter of 5.75 mm and an outer diameter of 7.9 mm. The tubes were made of soda–lime glass because of its relatively high fracture toughness. The same number of bases made of metallic sieves with an opening of 75 μm were prepared. These bases were circular and had a diameter that was 1 mm bigger than the outer diameter of the tube. Each base was glued to the bottom of a tube, which was sanded and cleaned beforehand. The glue was chosen for its high-temperature resistance and chemical resistance. One of the great advantages of this design is that the influence of the external meniscus, which occurs because of water moving upward along the external wall of the tube as a result of surface tension, is avoided (41). As shown in Figure 1, water is no longer able to form an external meniscus because of the existence of the metallic sieve. Also, the errors caused by the thick glass sieves used in previous studies were eliminated (10, 26).

Procedures

The following procedures were designed and strictly followed during the experiments:

1. All tubes and vessels were rinsed with acetone and then dried before tests.
2. The soils used for testing were dried in an oven (80°C) for 24 h. Then the soil specimens of Soil A or Sand B were prepared by following the previously mentioned procedures.

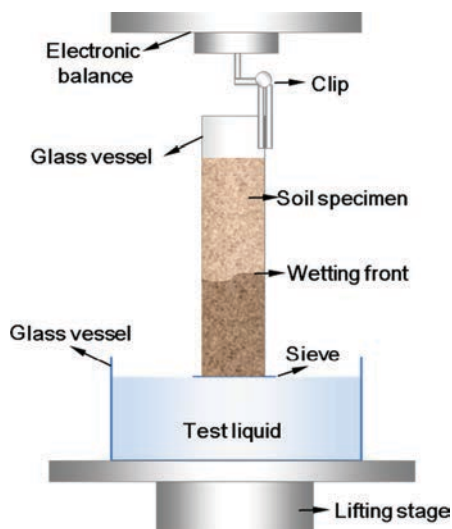


FIGURE 1 Instrument setup for CRM with Krüss 100 tensiometer.

3. The tube was put into the chamber of the tensiometer (Figure 1) and a rinsed vessel was filled with test liquid according to the requirement of the tensiometer.

4. The chamber was closed and a test started. Data are recorded as long as the specimen is in contact with the liquid. A measurement lasted a period of time ranging from 40 s to 120 s. This time depended on soil type and was determined by trial tests.

5. The procedure in Step 4 was repeated for another test. If a different test liquid was used, rinsing the vessel with acetone is necessary.

6. After an experiment, all tubes were cleaned and dried. Data were obtained for analysis.

Several issues require close attention during the process. First, clean gloves should be used throughout the whole process to protect the specimens from being contaminated by organic substances from hands. Second, aluminum foil was used under the bottoms of the tubes to protect the sieves. Moreover, all the specimens were covered with plastic wrap to make sure the dry specimens would not be moisturized by the humidity in the air. Finally, disturbances should be avoided during transport of the specimens.

RESULTS AND DISCUSSION

Method 1. Evaluation of Traditional CRM

The conventional CRM (Method 1) involves curve fitting a straight line in the measured m^2 - t curve. Experiments and analyses were performed first to evaluate its effectiveness and applicability for soils. Plotted in Figure 2 are the measured m^2 - t relationships for specimens made of Soil A and Sand B. For each soil, two specimens were tested with pentane and another two with water. The initial letters in the legend denote soil type (A or B), the following Arabic numbers represent the tube (specimen) number, and the last letters indicate the type of test liquid (P for pentane and W for water).

Comparisons between the results for the same soil measured with the same test liquid in the first type of experiment proved that the experiments have good repeatability. As can be seen, the two relevant curves measured with pentane for both soils and those measured with water for Sand B almost overlap. This finding indicates that the specimens prepared with the proposed procedures ensured that the conditions between specimens were similar. However, a relatively larger difference was found between the curves on the two specimens made of Soil A and measured with water. This difference is attributed to the differences in the internal structures (e.g., pore-size distribution and pore morphology) of the specimens.

Linear segments can be identified in some of the curves in Figure 2. These linear segments correspond to the phenomena prescribed by Method 1, for which inertia and gravity are neglected. Most of the previous applications of the CRM on soils are based on the identification of the gradient of this linear range. As can be seen, all of the curves in Figure 2a exhibit linearity after 10 s. For Sand B, there are also approximately linear segments for the curves measured with water between 2 to 5 s. However, it is difficult to find a linear part in the curves measured with pentane for Sand B. The phenomenon that a linear segment does not always evidently exist has also been observed in the experimental results for other specimens. In other words, Method 1 is not always applicable because the linearity predicted by the simplified Lucas–Washburn equation is difficult or even impossible to identify. Moreover, considerable

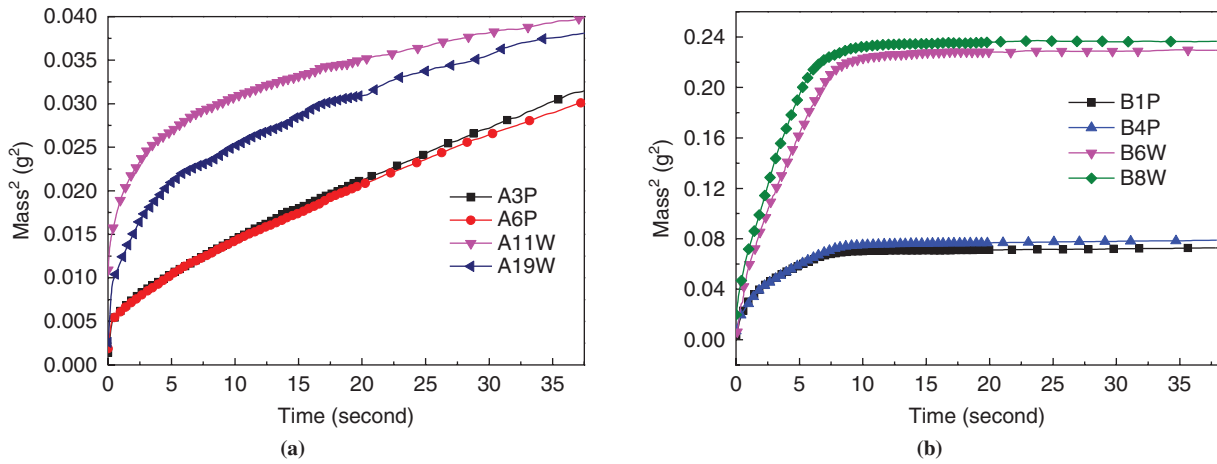


FIGURE 2 Measured m^2 - t relationship for (a) Soil A and (b) Sand B.

error could be produced by using Method 1 even when an obvious linear segment could be identified because of the fact that there is no criterion for locating the start and the end of this linear segment. Therefore, direct application of Method 1 as the conventional CRM is difficult for soils.

Method 2. Performance of Modified CRM

To improve the conventional CRMs, the solution to the Lucas-Washburn equation considering the gravity term that was developed by the authors (Equation 9) was further assessed. This modified CRM employs the corresponding analytical solution to fit the measured m - t curves. The value of κ_2 was obtained by using a nonlinear least squares curve fit method. MATLAB code was developed to automate the data processing.

Figure 3 shows typical examples of measured and fitted m - t curves for Soil A and Sand B using the modified CRM. As shown in Figure 3a, the measured and fitted curves almost coincide. This result indicates that the solution to the governing equation for the modified CRM describes the dynamics of capillary rise in these Soil A specimens very well. For Sand B, the comparison is still acceptable but not as good as that for Soil A specimens. Two possible rea-

sons for these differences were identified as follows: (a) the process of capillary rise is much faster in Sand B specimens than that in Soil A specimens; this difference could lead to more uncertainties and consequently a larger deviation from that predicted under ideal conditions; (b) the influence of inertia is relatively more significant (because of the faster speed of capillary rise) in the Sand B specimens yet not considered by the governing equation. The average apparent contact angle for the virgin Soil A specimens and virgin Sand B specimens are 89.43 degrees and 60.93 degrees.

It was reported that the influence of inertia is insignificant whenever \tilde{r} (effective radius in porous media) is smaller than the critical radius (28), r_c , which can be calculated by the following equations:

$$r_c = 2 \frac{(\gamma \cos(\theta) \eta^2 \rho^2 g^3)^{\frac{1}{5}}}{\rho g} \quad (16)$$

$$\tilde{r} = \left(\frac{16\alpha_2 \gamma_p \eta_p}{\rho_p^2 g^2} \right)^{\frac{1}{3}} \quad (17)$$

From Equation 17, the average effective radii for the specimens made of Soil A and Sand B are 8.51×10^{-3} mm and 7.23×10^{-2} mm,

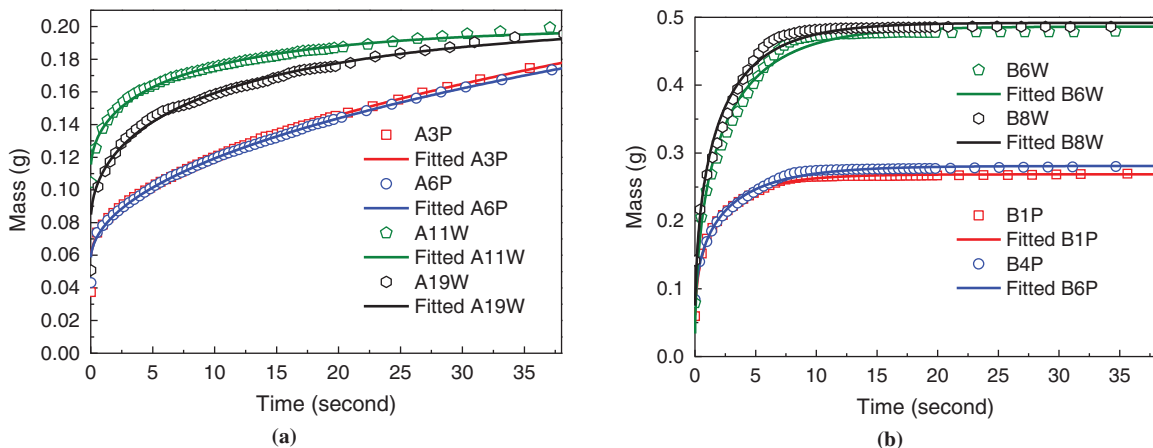


FIGURE 3 Examples of measured and fitted m - t curve for (a) virgin Soil A specimens and (b) Sand B specimens.

respectively. For both soils, the radii are much smaller than the critical radii as long as the apparent contact angle is less than 89.9 degrees. For the hydrophilic soils, the contact angle is usually much smaller than this value. So it is safe to apply Method 2 as long as the soil tested is not a coarse-grained soil with an approximately neutral wettability ($\theta = 90$ degrees). Under such a condition, the initial portion of the $m-t$ curve may need to be discarded before curve fitting.

Significance of Contact Angle to SWCC

The variations of contact angle with respect to the aggregate size for Soil A and Sand B are plotted in Figure 4. The radii were calculated with the sieve opening sizes in the analyses. The contact angle is an average value and corresponds to the group of soil that passes through the sieve of corresponding opening size. For Soil A, it is clear that contact angle increases as aggregate size decreases, whereas for Sand B, the contact angle increases at first and then decreases as aggregate size decreases. Factors responsible for the differences in the observed trends of contact angle variations with

particle radius in these two types of soils are unclear. The type of constituent mineral of the aggregates might be responsible for their behavior. Other factors include the roughness of particles and possible containment of organic materials (14, 42–45). These factors, however, need to be further investigated.

To evaluate the influence of contact angle on the construction of SWCCs, the experimental relationships between contact angle and particle size were fitted with continuous functions. The BiDoseResp function and fourth-order polynomial function embedded in a data analysis package, Origin, were used for Soil A and Sand B, respectively. As can be seen in Figure 4, satisfactory fitting results were obtained. In the next step, the relevance between the particle size distribution and pore-size distribution is taken advantage of according to the following equation proposed by Wu et al. (46):

$$r_o = R \left(\frac{O}{R} \right) \cdot r_R \tag{18}$$

where r_o and r_R are the radii of pores and particles, respectively. The experimental results of Wu et al. (46) based on seven soils suggested that $R(O/R)$ ranges from 0.25 to 2.26. Considering that the ratio of the average pore size of a group of sieved soils to the corresponding mesh size is less than 0.5 (Table 2), it is reasonable to assume that the radius given in Figure 4 equals the effective pore size. As a result, the relationship between contact angle and effective pore radius, $\theta(r)$, can be approximated by the obtained curve-fitting functions.

In traditional SWCC construction—for example, in the study by Fredlund et al. (7)—an SWCC is obtained by integrating the function of pore volume density, $f(r)$, with respect to pore size, r . In the current study, two ways of considering the contact angle were adopted to construct SWCCs based on the theory described by Fredlund et al. (7): (a) the assumption of perfect wettability (8) and (b) the relationships $\theta(r)$ obtained in this study. The pore-size distribution used for this study was measured by Lipiec et al. (47) with a mercury porosimeter, a technique based on the BCC model as well. This technique provides a way to assess the influence of the contact angle when SWCCs are constructed.

Plotted in Figure 5 are different SWCCs developed on the basis of the measured pore-size distribution either with consideration of the effects of the contact angle or not. Figure 5 shows the SWCCs constructed by assuming perfect wettability (contact angle of 0, which is commonly used in existing studies), the SWCCs constructed by using measured contact angle variation with pore radius for Soil A, and the SWCCs constructed by using measured contact angle variation with pore radius for Sand B. As shown in Figure 5a, the SWCC constructed with the contact angle for Soil A is significantly different from those obtained by assuming perfect wettability and by using the variation of contact angle for Sand B. In other words, there could be a large error in the estimate of the SWCC of the soil without considering the effects of contact angle. The difference for Soil A is obvious. There are also differences for Sand B, which are small but discernible with a closer look (Figure 5b). A difference of 25 kPa is identified for the total suction of about 180 kPa, which corresponds to a relative error of 13.99%. This finding provides a lower limit of the error, which could be caused by constructing SWCCs without considering the real variation of the contact angle with respect to pore size. Because Sand B consists mostly of silicon dioxide (99.7%), it has high surface energy and has rarely been contaminated by organic materials. It should have smaller contact angles than most of the soils encountered in geotechnical engineering practice. Therefore, the construction of the SWCC for this type of soil without considering contact angle should produce the smallest degree of error.

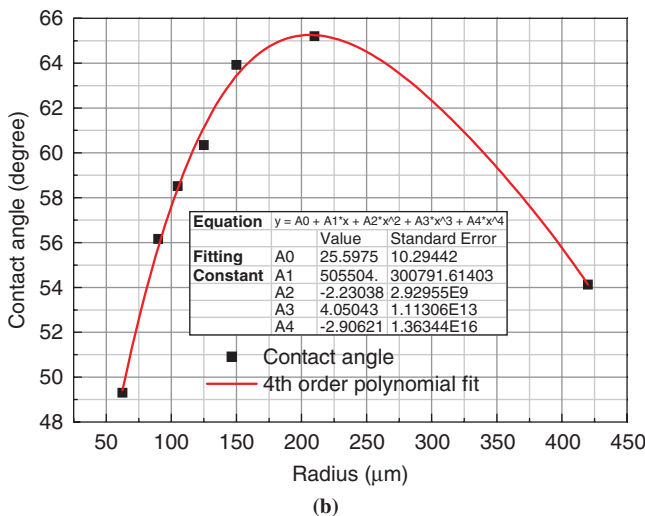
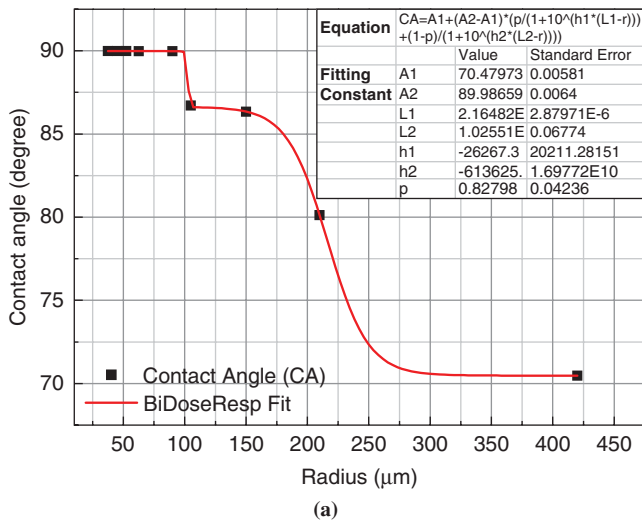


FIGURE 4 Contact angle versus particle radius (half of sieve opening) for (a) Soil A and (b) Sand B.

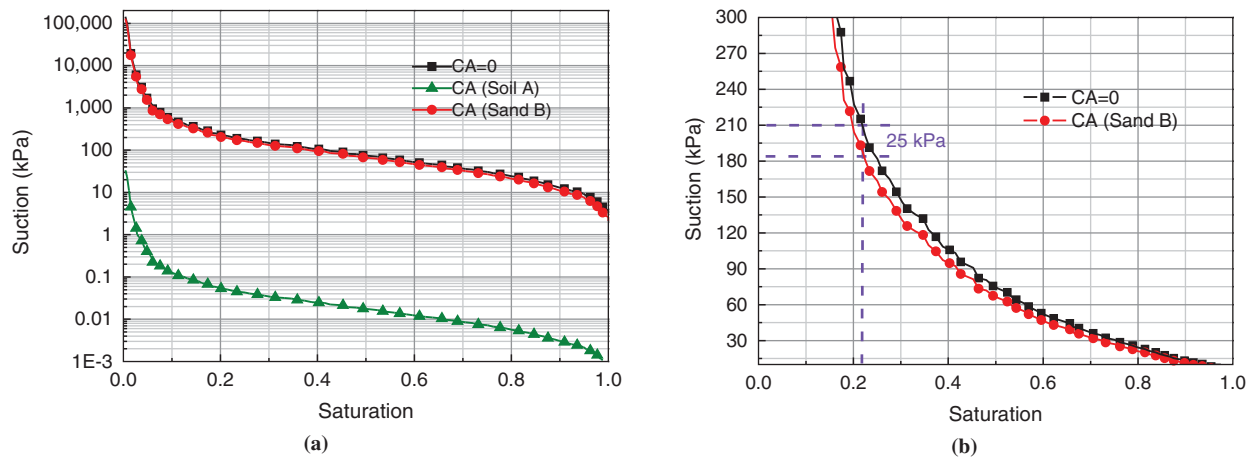


FIGURE 5 SWCCs constructed with different contact angle variations: (a) overall curves and (b) close-up view of curves.

CONCLUSION

A pioneering study on the measurement of contact angle and its relationship to the SWCC in geotechnical engineering practice is presented. The study first improved the procedures and analysis for the CRM for measuring the contact angles of soils. Experiments were conducted to measure the variations of contact angle with pore radius for different types of soils. Then the effects of contact angle on the estimation of the SWCCs were studied. The results indicated that contact angle could have a major effect on the SWCCs; this factor needs to be considered for the estimation of SWCCs from the pore-size distribution.

ACKNOWLEDGMENTS

The authors acknowledge Adin Mann and Vladimir Gurau in the Department of Chemical Engineering at Case Western Reserve University for the inspiring discussions on contact angle measurements with the CRM and for access to the surface engineering instruments.

REFERENCES

- Lu, N., and W. J. Likos. *Unsaturated Soil Mechanics*. John Wiley and Sons, New York, 2004.
- Anderson, M. A., A. Y. C. Hung, D. Mills, and M. S. Scott. Factors Affecting the Surface Tension of Soil Solutions and Solutions of Humic Acids. *Soil Science*, Vol. 160, No. 2, 1995, pp. 111–116.
- Doerr, S. H., R. A. Shakesby, and R. P. D. Walsh. Soil Water Repellency: Its Causes, Characteristics and Hydro-Geomorphological Significance. *Earth Science Review*, Vol. 51, No. 1, 2000, pp. 33–65.
- Bachmann, J., and R. R. van der Ploeg. A Review on Recent Developments in Soil Water Retention Theory: Interfacial Tension and Temperature Effects. *Journal of Plant Nutrition and Soil Science*, Vol. 165, No. 4, 2002, pp. 468–478.
- Grant, S. A., and A. Salehzadeh. Calculation of Temperature Effects on Wetting Coefficients of Porous Solids and Their Capillary Pressure Functions. *Water Resources Research*, Vol. 32, No. 2, 1996, pp. 261–270.
- Lety, J., J. Osborn, and R. E. Pelishek. Measurement of Liquid Solid Contact Angles in Soil and Sand. *Soil Science*, Vol. 93, No. 3, 1962, pp. 149–153.
- Fredlund, D. G., A. Xing, and S. Huang. Predicting the Permeability Function for Unsaturated Soils Using the Soil–Water Characteristic Curve. *Canadian Geotechnical Journal*, Vol. 31, No. 4, 1994, pp. 533–546.
- Arya, L. M., and J. F. Paris. A Physicoempirical Model to Predict Soil Moisture Characteristics from Particle-Size Distribution and Bulk Density Data. *Soil Science Society of America Journal*, Vol. 45, No. 6, 1981, pp. 1023–1030.
- Drelich, J., and J. D. Miller. The Effect of Solid Surface Heterogeneity and Roughness on the Contact Angle–Drop (Bubble) Size Relationship. *Journal of Colloid and Interface Science*, Vol. 164, No. 1, 1994, pp. 252–259.
- Goebel, M.-O., J. Bachmann, S. K. Woche, W. R. Fischer, and R. Horton. Water Potential and Aggregate Size Effects on Contact Angle and Surface Energy. *Soil Science Society of America Journal*, Vol. 68, No. 2, 2004, pp. 383–393.
- Grant, S. A., and J. Bachmann. Effect of Temperature on Capillary Pressure. *Geophysical Monograph*, Vol. 129, 2002, pp. 199–212.
- Quere, D. Wetting and Roughness. *Annual Review of Materials Research*, Vol. 38, 2008, pp. 71–99.
- Ramirez-Flores, J., S. K. Woche, J. Bachmann, M.-O. Goebel, and P. D. Hallett. Comparing Capillary Rise Contact Angles of Soil Aggregates and Homogenized Soil. *Geoderma*, Vol. 146, No. 1–2, 2008, pp. 336–343.
- Dekker, L. W., and C. J. Ritsema. Wetting Patterns and Moisture Variability in Water Repellent Dutch Soils. *Journal of Hydrology*, Vol. 231, 2000, pp. 148–164.
- King, P. M. Comparison of Methods for Measuring Severity of Water Repellence of Sandy Soils and Assessment of Some Factors That Affect Its Measurement. *Australian Journal of Soil Research*, Vol. 19, No. 3, 1981, pp. 275–285.
- De Jonge, L. W., O. H. Jacobsen, and P. Moldrup. Soil Water Repellency: Effects of Water Content, Temperature, and Particle Size. *Soil Science Society of America Journal*, Vol. 63, No. 3, 1999, pp. 437–442.
- Niggemann, J. Versuche zur Messung der Benetzungsfähigkeit von Torf. *Torfnachrichten*, Vol. 20, 1970, pp. 14–18.
- Reeker, R. Die Benetzungsfähigkeit von Torfmüll. *Torfnachrichten*, Vol. 7, 1954, pp. 15–16.
- Adamson, A. W. *Physical Chemistry of Surfaces*, 5th ed. John Wiley and Sons, New York, 1990.
- Bachmann, J., R. Horton, R. R. van der Ploeg, and S. K. Woche. Modified Sessile Drop Method for Assessing Initial Soil-Water Contact Angle of Sandy Soil. *Soil Science Society of America Journal*, Vol. 64, No. 2, 2000, pp. 564–567.
- Bachmann, J., S. K. Woche, M.-O. Goebel, M. B. Kirkham, and R. Horton. Extended Methodology for Determining Wetting Properties of Porous Media. *Water Resources Research*, Vol. 39, No. 12, 2004, p. 1353.
- Lucas, R. Rate of Capillary Ascension of Liquids. *Kolloid Zeitschrift*, Vol. 23, 1918.
- Washburn, E. W. The Dynamics of Capillary Flow. *Physical Review*, Vol. 17, No. 3, 1921, pp. 273–283.
- Tuller, M., D. Or, and L. M. Dudley. Adsorption and Capillary Condensation in Porous Media: Liquid Retention and Interfacial Configurations in Angular Pores. *Water Resources Research*, Vol. 35, No. 7, 1999, pp. 1949–1964.
- Siebold, A., A. Walliser, M. Nardin, M. Oppliger, and J. Schultz. Capillary Rise for Thermodynamic Characterization of Solid Particle Surface. *Journal of Colloid and Interface Science*, Vol. 186, No. 1, 1997, pp. 60–70.

26. Michel, J.-C., L.-M. Riviere, and M.-N. Bellon-Fontaine. Measurement of the Wettability of Organic Materials in Relation to Water Content by the Capillary Rise Method. *European Journal of Soil Science*, Vol. 52, No. 3, 2001, pp. 459–467.
27. Abu-Zreig, M., R. P. Rudra, and W. T. Dickinson. Effect of Application of Surfactants on Hydraulic Properties of Soils. *Biosystems Engineering*, Vol. 84, No. 3, 2003, pp. 363–372.
28. Hamraoui, A., and T. Nylander. Analytical Approach for the Lucas–Washburn Equation. *Journal of Colloid and Interface Science*, Vol. 250, No. 2, 2002, pp. 415–421.
29. Zhmud, B. V., F. Tiberg, and K. Hallstenson. Dynamics of Capillary Rise. *Journal of Colloid and Interface Science*, Vol. 228, No. 2, 2000, pp. 263–269.
30. Schoelkopf, J., P. A. C. Gane, C. J. Ridgway, and C. P. Matthews. Practical Observation of Deviation from Lucas–Washburn Scaling in Porous Media. *Colloids and Surfaces A: Physicochemical and Engineering Aspects*, Vol. 206, No. 1–3, 2002, pp. 445–454.
31. Levine, S., J. Lowndes, E. J. Watson, and G. Neale. A Theory of Capillary Rise of a Liquid in a Vertical Cylindrical Tube and in a Parallel-Plate Channel. *Journal of Colloid and Interface Science*, Vol. 73, No. 1, 1980, pp. 136–151.
32. Fries, N., and M. Dreyer. The Transition from Inertial to Viscous Flow in Capillary Rise. *Journal of Colloid and Interface Science*, Vol. 327, No. 1, 2008, pp. 125–128.
33. Barry, D. A., J.-Y. Parlange, L. Li, H. Prommer, C. J. Cunningham, and F. Stagnitti. Analytical Approximations for Real Values of the Lambert W-function. *Mathematics and Computers in Simulation*, Vol. 53, No. 1–2, 2000, pp. 95–103.
34. Czachor, H. Modelling the Effect of Pore Structure and Wetting Angles on Capillary Rise in Soils Having Different Wettabilities. *Journal of Hydrology*, Vol. 328, No. 3–4, 2006, pp. 604–613.
35. Grundke, K. Wetting, Spreading and Penetration. In *Handbook of Applied Surface and Colloid Chemistry* (K. Holmberg, ed.), John Wiley and Sons, New York, 2002.
36. Morrow, N. R. Physics and Thermodynamics of Capillary. *Industrial and Engineering Chemistry*, Vol. 62, No. 6, 1970, pp. 32–56.
37. Dullien, F. A. L., M. S. El-Sayed, and V. K. Batra. Rate of Capillary Rise in Porous Media with Nonuniform Pores. *Journal of Colloid Science*, Vol. 60, No. 3, 1977, pp. 497–506.
38. Vorvort, R. W., and S. R. Cattle. Linking Hydraulic Conductivity and Tortuosity Parameters to Pore Space Geometry and Pore-Size Distribution. *Journal of Hydrology*, Vol. 272, No. 1, 2003, pp. 36–49.
39. Gurau, V., and J. A. Mann. Technique for Characterization of the Wettability Properties of Gas Diffusion Media for Proton Exchange Membrane Fuel Cells. *Journal of Colloid and Interface Science*, Vol. 350, No. 2, 2010, pp. 577–580.
40. *Krüß Tensiometer 100 Instruction Manual V020715*. Krüss GmbH, Hamburg, Germany, 2001.
41. Friess, B. R., and M. Hoorfar. Measurement of Internal Wettability of Gas Diffusion Porous Media of Proton Exchange Membrane Fuel Cells. *Journal of Power Sources*, Vol. 195, No. 5, 2010, pp. 4736–4742.
42. Oades, J. M. The Retention of Organic Matter in Soils. *Biogeochemistry*, Vol. 5, No. 1, 1988, pp. 35–70.
43. Ducarior, J., and I. Lamy. Evidence of Trace Metal Association with Soil Organic Matter Using Particle Size Fractionation After Physical Dispersion Treatment. *Analyst*, Vol. 120, No. 3, 1995, pp. 741–745.
44. Ryan, B. J., and K. M. Poduska. Roughness Effects on Contact Angle Measurements. *American Journal of Physics*, Vol. 76, No. 11, 2008, pp. 1074–1077.
45. Tamai, Y., and K. Aratani. Experimental Study of the Relation Between Contact Angle and Surface Roughness. *Journal of Physical Chemistry*, Vol. 76, No. 22, 1972, pp. 3267–3271.
46. Wu, L., J. A. Vomocil, and S. W. Childs. Pore Size, Particle Size, Aggregate Size, and Water Retention. *Soil Science Society of America Journal*, Vol. 54, No. 4, 1990, pp. 952–956.
47. Lipiec, J., M. Hajnos, and R. Swieboda. Estimating Effects of Compaction on Pore Size Distribution of Soil Aggregates by Mercury Porosimeter. *Geoderma*, Vols. 179–180, 2012, pp. 20–27.

The Engineering Behavior of Unsaturated Soils Committee peer-reviewed this paper.